Novel Destabilization of Nucleotide Binding by the γ Phosphate of ATP in the Yeast SR Protein Kinase Sky1p†

Brandon E. Aubol,‡ Brad Nolen,‡ Jennifer Shaffer,§ Gourisankar Ghosh,‡ and Joseph A. Adams*,§

Departments of Pharmacology and Chemistry and Biochemistry, University of California, San Diego, La Jolla, California 92093-0506

Received July 9, 2003; Revised Manuscript Received August 22, 2003

ABSTRACT: SR protein kinases (SRPKs) regulate the temporal and cell-specific selection of alternative splice sites. These enzymes are highly unique members of the protein kinase family. SRPKs contain a large domain insert (approximately 200 residues) within the kinase core, do not require phosphorylation for regulation, have an extended helix insert near the nucleotide pocket, and possess unusual substrate specificity determinants. The yeast SRPK, Sky1p, rapidly phosphorylates its natural substrate Npl3 but binds ATP with a high K_m, suggesting that some of these distinctive structural features may be correlated with nucleotide binding [Aubol et al. (2002) *Biochemistry 41*, 10002−10009]. To address this issue, the nucleotide binding properties of Sky1p were studied using fluorescence spectroscopy. The affinities of several nucleotides (ATP, ADP, AMP, adenosine, and AMPPNP) to Sky1p and the prototype kinase, cAMP-dependent protein kinase, were compared in the absence and presence of the metal activator, Mg^{2+}, using a fluorescence-based displacement assay. The data indicate that Sky1p, unlike cAMP-dependent protein kinase, potently destabilizes the γ phosphate of ATP. This novel finding suggests that rapid phosphoryl transfer may be facilitated by unique mechanisms in both protein kinases.

Protein kinases play key roles in numerous cellular processes, such as gene expression, immune responses, inflammation, apoptosis, metabolic regulation, and pre-mRNA splicing. Not surprisingly, abnormal protein kinase activity is often associated with human ailments including cancer, antibiotic resistance, neurodegenerative diseases, and depression (*1*−*4*). The clear connection between protein kinases and disease has fueled many investigations into kinase-directed drugs. To date, two protein kinase inhibitors, Gleevec (STI-571) and rapamycin, are in clinical use for the treatment of chronic myelogeneous leukemia and tissue rejection after organ transplantation, respectively (*5*). While this represents a small number of approved drugs, many are currently in human clinical phase trials and show good promise for the treatment of a wide variety of disorders (*6*−*8*). Although rapamycin utilizes a unique mechanism (*9*), Gleveec and the vast majority of these potential drugs target the active site by competing with ATP (*7*). Despite the fact that the ATP binding site is largely conserved across the kinase family, key variations exist in the architecture of the regions proximal to this site that allow selective toxicity (*7*).

It has been estimated that 15% of all nucleotide substitutions leading to human disease are the result of aberrant pre-mRNA splicing (*4*). Eukaryotic pre-mRNA splicing is the process whereby mature mRNA is formed by removing the noncoding sequences (introns) from coding sequences (exons) in pre-mRNA molecules (*10*). This process is carried out by a cellular machine known as the spliceosome, a large dynamic assembly of small nuclear RNAs (snRNAs),[1] small ribonuclear proteins (snRNPs), and many non-snRNPs (*10*−*13*). The catalytic core of the spliceosome is formed through a series of RNA−RNA interactions that are facilitated by the nonsnRNP components of the spliceosome (*14*), most notably SR proteins. SR proteins are the most well-characterized of the nonsnRNP molecules and function to modulate splice site selection and spliceosome assembly in a phosphorylation-dependent manner (*15*). In fact, eukaryotic splicing occurs within a dynamic cycle of phosphorylation and dephosphorylation events critical for the proper formation of mature mRNA with a high fidelity (*14*, *16*, *17*).

The phosphorylation of SR proteins is carried out by a class of enzymes known as SR protein kinases (SRPKs) (*18*−*21*). SRPKs are highly homologous across species (∼50% identity between human and yeast) and are characterized by a large insert of ∼250−300 residues (spacer region) in the kinase core. This spacer region is critical for subcellular localization and cell viability in yeast (*22*). In *Saccharomyces cerevisiae*, Sky1p has been identified as the only kinase highly homologous to human SRPKs. Although there exist multiple substrates that can be phosphorylated by Sky1p in yeast, Npl3p is the only one that is well-characterized (*22*).

† This work was supported by an NSF (111068) and NIH grant (GM 68168). B.E.A. was supported by an NIH training grant (GM 07752).

* Corresponding author. Tel: (858) 822-3360. Fax: (858) 822-3361. E-mail: joeadams@ucsd.edu.

‡ Department of Chemistry and Biochemistry.

§ Department of Pharmacology.

[1] Abbreviations: AMPPNP, 5-adenylylimido diphosphate; MANT, *N*-methylanthraniloyl; MANT-ADP, ADP with MANT attached to ribose ring; MANT-ATP, ATP with MANT attached to ribose ring; PKA, cAMP-dependent protein kinase; Sky1p, SR protein kinase in yeast; Sky1pΔNS, Sky1p lacking the spacer insert and N-terminus; snRNA, small nuclear RNAs; snRNP, small nuclear ribonuclear protein; SRPK, SR protein kinase; SR protein, splicing factor containing arginine−serine dipeptide repeats.

10.1021/bi035200c CCC: $25.00 © 2003 American Chemical Society
Published on Web 10/18/2003

Npl3p has characteristics of both the hnRNP and the SR protein subfamilies and has been implicated in mRNA transport from the nucleus to the cytoplasm (*23*).

All members of the SRPK family, including Sky1p, show a high degree of substrate specificity and are constitutively active (*18*, *20*, *21*, *24*, *25*). The recently solved structure of Sky1p lacking this spacer region and a large portion of the N-terminus (Sky1pΔNS) has revealed that this enzyme differs from other protein kinases in two ways (*26*). First, Sky1p is not regulated through activation loop phosphorylation, but rather this critical loop segment is locked into a productive form by a direct interaction with the C-terminal tail. Second, Sky1p contains a short helical addition directly following helix αC. Since it has been demonstrated in other kinases that motions in helix αC are directly linked to catalytic activation and productive nucleotide binding (*27*−*29*), the presence of this helical insert suggests a unique role in SRPKs.

Despite broad interest in the protein kinases as drug targets and the current exploitation of the nucleotide pocket to achieve selective inhibition, there are few structure−function studies on this region of the active site. In a previous investigation, we showed that Sky1p binds ATP and its physiological substrate, Npl3p, randomly although the K_m for ATP is uncharacteristically high as compared to other protein kinases (*30*−*32*). Regardless of the apparent inefficient binding of ATP, Npl3p is rapidly phosphorylated in the active site so that turnover is limited by product release and/or associated conformational changes (*24*). The recent X-ray structure of Sky1p with ATP and ADP bound indicated that the degree of hydrogen bonding and lobe closure in the two structures is distinctly different, suggesting that ATP and ADP may bind with different affinities (*33*). To probe the topology of the nucleotide pocket in Sky1p, we designed a fluorescence-based displacement assay to determine the dissociation constants of a wide range of nucleotides (ATP, ADP, AMP, adenosine, and AMPPNP) to Sky1p. We found that nucleotides are stabilized in the active site by a novel mechanism that noticeably differs with that utilized by the protypical serine/threonine kinase, cAMP-dependent protein kinase (PKA). Unlike PKA, Sky1p strongly destabilizes the γ phosphate of ATP without impairing the efficient phosphoryl transfer step.

MATERIALS AND METHODS

Materials. Adenosine triphosphate (ATP), adenosine diphosphate (ADP), adenosine monophosphate (AMP), adenosine (Ad), 3-(*N*-morpholino)propanesulfonic acid (MOPS), magnesium chloride, acetic acid, DE52 resin, EDTA, and liquid scintillant were obtained from Fisher Scientific. Poly-prep chromatography columns were obtained from Bio-Rad, synthetic peptide was obtained from the peptide and oligonucleotide facility at the University of Southern California, 5-adenylylimido diphosphate (AMPPNP) was obtained from Sigma Chemicals, *N*-methylanthraniloyl (MANT) fluorophores were obtained from Molecular Probes, and [γ-^{32}P] ATP was obtained from NEN Products. Recombinant proteins, Sky1pΔNS, Sky1p full length, and Npl3 were expressed in *Escherichia coli* and purified according to previously reported procedures (*24*, *26*). PKA was expressed and purified using previously published procedures (*34*). Concentration measurements for the purified proteins were made using the Gill and von Hippel method (*35*).

Equilibrium Fluorescence Spectroscopy. Fluorescence experiments were carried out on the Flouromax-2 (Jobin Yvon-SPEX, Instruments S. A., Inc. Edison, NJ) equipped with a circulating water bath and a 300 μL cuvette and holder. The binding of the MANT-nucleotide derivatives was monitored by preparing a 300 μL sample containing 25 μM MANT-ADP, in 50 mM MOPS (pH 7.0), and 4 mM free Mg^{2+}. Emission spectra between 300 and 550 nm were then acquired by exciting the samples at 290 nm (excitation and emission slits were set to 2 and 2 nm, respectively). Sky1pΔNS was next added directly to the cuvette to a final concentration of 1 μM, and the fluorescence spectra were reacquired. Finally, either 5 mM ATP or 1 mM ADP was added to monitor the MANT nucleotide displacement from the active site. Control experiments were carried out in the absence of Sky1pΔNS to ensure that ADP and ATP did not alter the fluorescence emission of the MANT nucleotides, and all spectral intensities were corrected for dilution.

MANT Nucleotide Affinities. Titrations of MANT-ATP and MANT-ADP were carried out in 50 mM MOPS (pH 7.0), 4 mM free Mg^{2+}, and 1 μM Sky1pΔNS unless otherwise stated. Microliter quantities of MANT-ATP and MANT-ADP were added to 300 μL samples from stock solutions of fluorescent nucleotide. MANT-ATP and MANT-ADP concentrations were measured spectrophotometrically (ϵ_{356} = 5800 cm^{-1} M^{-1}). Changes in fluorescence intensity were monitored by obtaining emission spectra between 300 and 550 nm by excitation at 290 nm (excitation and emission slits were set to 2 nm) as a function of increasing MANT nucleotide concentration. A background sample titration lacking Sky1pΔNS was carried out for each titration of MANT nucleotide in the presence of protein. For the measurement of dissociation constants for adenosine, AMP, ADP, AMPPNP, and ATP, titrations were carried out as described previously in the presence of the competing nucleotide.

HPLC Detection of Substrate Phosphorylation. The phosphorylation of the peptide substrate, YRTRDAPRERSPTR, by Sky1pΔNS using MANT-ATP was monitored using HPLC detection. Assays were performed in the presence of 1 μM Sky1pΔNS, 1 mM peptide, and 4 mM free Mg^{2+}, with either 1 mM MANT-ATP or 1 mM ATP in a total volume of 3 mL. These mixtures were allowed to react in 50 mM MOPS (pH 7.0) at 23 °C, and aliquots (400 μL) were removed at various time points, quenched by the addition of 25 μL of 0.5 M EDTA, and frozen prior to analysis. A portion of the quenched samples (200 μL) was injected and eluted from a reversed-phased column (Waters RCM or Vydac) using a linear gradient of 5−30% acetonitrile in 0.1% TFA, and the amount of phosphopeptide formed was recorded using an absorbance of 214 nm.

Enzyme Assays. Steady-state kinetic parameters in the presence of either protein substrate Npl3p or substrate peptide were determined at 23 °C for 2 min in the presence of 50 mM MOPS (pH 7.0), 4 mM free Mg^{2+}, and [γ-^{32}P]ATP (600−1000 cpm $pmol^{-1}$) unless otherwise stated. Initial velocities were determined from progress curves of ^{32}P versus time. For inhibition studies, substrate concentrations were kept constant at various inhibitor concentrations. Assays were typically executed by preequilibrating the enzyme, $MgCl_2$,

and ATP for 2 min, then initiating the reaction with the addition of substrate. Total reaction volumes were 20 μL and were quenched with 180 μL of 30% acetic acid. A portion of each reaction (180 μL) was applied to 3 mL DE52 columns and washed with 5 mL of 30% acetic acid. The collected flow, although containing phosphorlyated substrate, was then counted on the ^{32}P channel in liquid scintillant. Control experiments were performed to determine the background phosphorylation (i.e., phosphorylation of Npl3p or substrate peptide in the presence of quench). The specific activity of [γ-^{32}P] ATP was determined by measuring the total counts of the reaction mixture. The time-dependent concentration of phosphorylated Npl3p and substrate peptide was then determined by considering the total counts per minute (CPM) of the flow through, the specific activity of the reaction mixture, and the background phosphorylation of the flow through as previously described.

Data Analysis. The observed changes in fluorescence intensity at any given concentration of MANT nucleotide (ΔF) were normalized against the total change in fluorescence at infinite concentration of MANT nucleotide (ΔF_{max}) to obtain the ratio $\Delta F/\Delta F_{max}$. Data were fit using the hyperbolic eq 1

$$\Delta F/\Delta F_{max} = \frac{[MANT]}{K_d^{MANT} + [MANT]} \quad (1)$$

where K_d^{MANT} is the K_d for the MANT nucleotide, and [MANT] is the concentration of the MANT nucleotide. For MANT-ADP titration experiments in the presence of fixed amounts of competing nucleotides, the plots yield apparent K_d values for MANT-ADP ($^{app}K_d^{MANT}$). The true K_d values for the competing ligands were then calculated using eq 2

$$^{app}K_d^{MANT} = K_d^{MANT}\left(1 + \frac{[L]}{K_d^L}\right) \quad (2)$$

where [L] and K_d^L are the concentration and dissociation constants for the competing nucleotide. For the inhibition studies, the K_I for the competing nucleotides was measured using fixed ATP and Npl3p concentrations using eq 3

$$v = \frac{V_{max}[ATP]}{K_{ATP}\left(1 + \frac{[AMPPNP]}{K_I}\right) + [ATP]} \quad (3)$$

where V_{max} is the maximal velocity in the absence of inhibitor, K_{ATP} represents the K_m for ATP, and K_I is the inhibitory constant for the competing nucleotide.

RESULTS

MANT Nucleotide Fluorescence Is Enhanced by Binding to Sky1pΔNS. As shown in Figure 1, the emission maximum for MANT-ATP at 440 nm increases in the presence of Sky1pΔNS. This fluorescence enhancement is reversed with the addition of the natural nucleotide ATP as well as ADP (data not shown). Since only a small amount of fluorescence above 400 nm is observed due to the intrinsic fluorescence of Sky1pΔNS (1 μM), the large enhancement at 440 nm upon MANT-ATP binding has no contributions from the Sky1pΔNS spectra. Similar spectra were recorded for MANT-ADP with

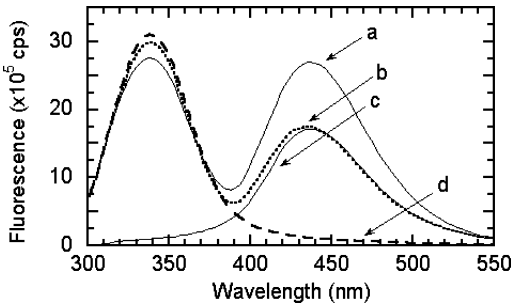

FIGURE 1: Effects of Sky1pΔNS on the fluorescence spectra of MANT-ATP. Spectra of MANT-ATP with Sky1pΔNS (a), MANT-ATP with Sky1pΔNS in the presence of 5 mM ATP (b), MANT-ATP alone (c), and Sky1pΔNS alone (d). Excitation wavelength is 290 nm, and the excitation and emission slits are both set at 2 nm. The concentrations of MANT-ATP, Sky1pΔNS, and free Mg^{2+} are 25 μM, 1 μM, and 4 mM, respectively, in all spectra. The fluorescence output is expressed as units of cps (counts per second).

a nearly identical observed increase in fluorescence at 440 nm upon the association of the enzyme (data not shown). To determine whether any of the fluorescence enhancement is due to energy transfer between tryptophan and the MANT group, excitation spectra in the absence and presence of enzyme at the same concentrations as those in Figure 1 were recorded (data not shown). As observed previously for MANT-derivatives (*36*), two maxima at 253 and 355 nm were detected in the excitation spectra. The absence of an excitation peak at the protein absorption maximum (290 nm) suggests that the fluorescence change at 440 nm in Figure 1 is most likely due to direct enhancement of the MANT fluorophore upon protein association. The ability to excite the MANT group away from its maximum at 340 nm minimizes background fluorescence at 440 nm from unbound fluorescent nucleotide in titration experiments.

MANT Derivatives Bind with Good Affinity to Sky1pΔNS. The dissociation constants for the MANT nucleotide derivatives were measured using increases in MANT fluorescence resulting from association with the enzyme. In these experiments, MANT spectra were recorded in the presence and absence of Sky1pΔNS, and the change in relative fluorescence at 440 nm was recorded and corrected for intrinsic Sky1pΔNS fluorescence. Plots of the relative change in fluorescence intensity ($\Delta F/\Delta F_{max}$) for MANT-ATP and MANT-ADP are plotted as a function of fluorescent nucleotide concentration in Figure 2. These data are fit to eq 1 to provide K_d values of 12 $\pm$ 1.5 μM for MANT-ADP and 13 $\pm$ 3 μM for MANT-ATP. The fluorescence intensity for MANT-ADP and MANT-ATP in the absence of Sky1pΔNS increased linearly with the concentration of nucleotide (data not shown), indicating that the curvature of the plots shown in Figure 2 is not due to the saturation of the detector. The data show that the addition of the fluorophore to the 2′(3′) hydroxyl of the ribose ring generates nucleotide probes with good binding affinity for the Sky1p active site.

MANT-ATP Is a Poor Substrate for Sky1pΔNS. The ability of MANT-ATP to act as a viable phosphate donor for Sky1pΔNS was determined using HPLC methods. Sky1pΔNS (1 μM) was mixed with the peptide substrate YRTRDAPRERSPTR (1 mM) and either MANT-ATP (1 mM) or ATP (1 mM) in the presence of 4 mM free Mg^{2+}. At various times, the reaction mixtures were quenched with the addition of 0.5 M EDTA and then injected onto the HPLC

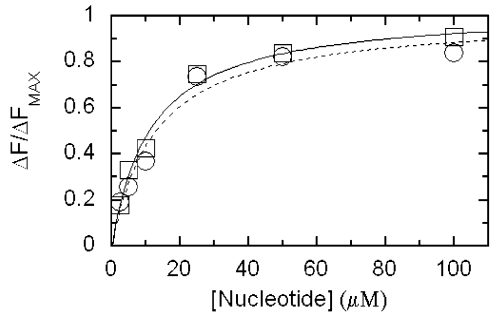

FIGURE 2: Change in fluorescence emission as a function of MANT-ADP (□) and MANT-ATP (○) concentration. The spectra of MANT nucleotide and Sky1pΔNS alone were subtracted from the spectra of MANT nucleotide with Sky1pΔNS. The observed changes in fluorescence intensity at any given concentration of MANT nucleotide at 440 nm (ΔF) were normalized against the total change in fluorescence at infinite concentration of MANT nucleotide (ΔF_{max}) to obtain the ratio $\Delta F/\Delta F_{max}$. This ratio was plotted as a function of MANT nucleotide concentration using 1 μM Sky1pΔNS in all spectra. The data were fit to eq 1 to obtain K_d values for MANT-ADP (12 ± 1.5 μM) and MANT-ATP (13 ± 3.0 μM).

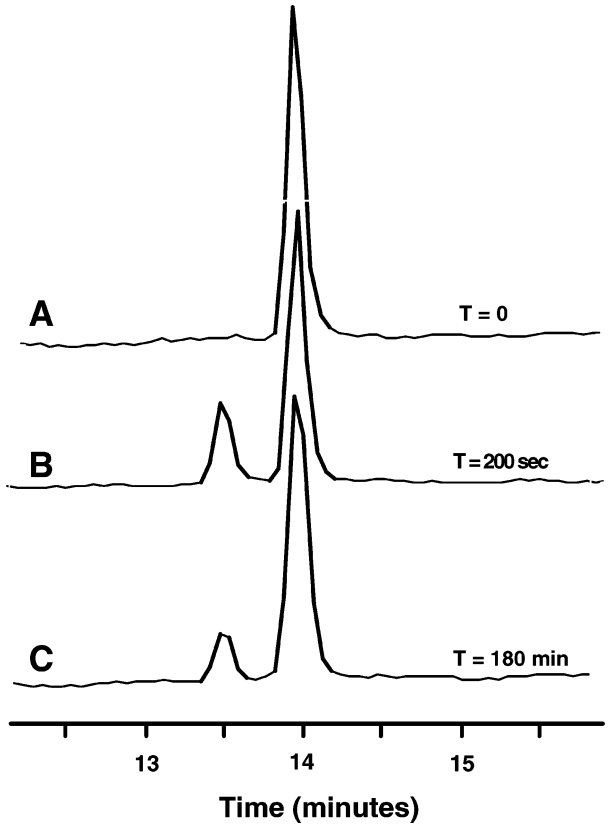

FIGURE 3: Phosphorylation of a peptide substrate by Sky1pΔNS using ATP or MANT-ATP. (A) Sky1pΔNS is mixed with peptide YRTRDAPRERSPTR and injected onto the HPLC column. (B) Sky1pΔNS is mixed with peptide and ATP, allowed to incubate for 200 s, and then injected onto the column. (C) Sky1pΔNS is mixed with peptide and MANT-ATP, allowed to react for 180 min, and injected onto the column.

column. Chromatographs of the reactions after the first 200 s with ATP and 180 min with MANT-ATP are shown in Figure 3 for comparison. The unphosphorylated peptide peak was assigned based on injecting a purified peptide sample alone onto the HPLC (Figure 3A). The appearance of a new peak shown in Figure 3B,C is time dependent (data not shown) and is accompanied by a decrease in the area of the unphosphorylated peptide peak, suggesting that the new peak corresponds with the phosphopeptide. The integrated areas of the peaks (detection at 214 nm) were used to determine the concentrations of the phosphorylated and the unphosphorylated peptide. As shown in Figure 3, the phosphotransfer reaction using MANT-ATP occurs 60 times slower (0.8 μM/min) relative to ATP (48 μM/min). Thus, while MANT-ATP binds well in the active site, it does not serve as a good phosphoryl donor in the active site of Sky1pΔNS. The reason for this is unclear at this point. While MANT-ATP and MANT-ADP bind with similar affinities, we will show that the natural nucleotides do not. The molecular underpinnings of this unusual selectivity and catalytic activity await an X-ray structure of Sky1pΔNS with the MANT nucleotides bound.

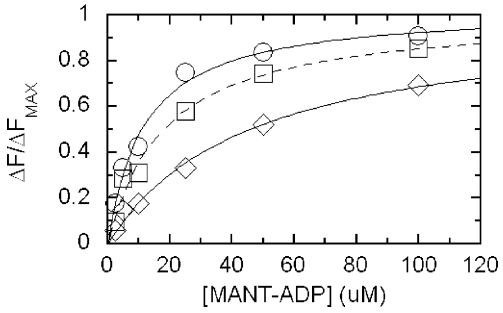

FIGURE 4: Fluorescence displacement assay. Relative changes in MANT-ADP fluorescence are monitored upon the addition of Sky1pΔNS (1 M) in the absence (○) and presence of 100 M ADP (◇) and 1 mM ATP (□). The data were fit to eq 1, and natural nucleotide K_d values were determined using eq 2 and are listed in Table 1. The free Mg^{2+} concentration is 4 mM in all experiments.

Affinities of Natural Nucleotides Can Be Measured using a Displacement Assay. Since MANT-ATP is a poor substrate for Sky1p and binds unproductively, we used a fluorescence displacement assay to determine the affinities of ATP and other nonderivatized nucleotides. These experiments were performed by monitoring the effects of natural nucleotides on the apparent K_d ($^{app}K_d^{MANT}$) for MANT-ADP. Figure 4 shows binding curves for MANT-ADP in the absence and presence of ADP (100 μM) and ATP (1 mM). As expected, both ATP and ADP increase the concentration of MANT-ADP required to saturate the enzyme and provide a maximum fluorescence enhancement. The $^{app}K_d$ values for MANT-ADP in the presence of ADP and ATP (Figure 4) are 40 ± 7 and 18 ± 3 μM, respectively. Using eq 2, K_d, and $^{app}K_d^{MANT}$ for MANT-ADP, the dissociation constants for several nucleotides were calculated (Table 1). While the $^{app}K_d^{MANT}$ for MANT-ADP in the presence of 1 mM ATP is statistically different than the true MANT-ADP K_d (12 ± 1.5 μM, Table 2), they are close in value. This indicates that the K_d for ATP is difficult to measure with high precision since we are unable to go higher than 1 mM of the competing natural nucleotide owing to quenching due to inner filter effects. For comparison, we also measured the K_I values of these nucleotides using fixed, saturating concentrations of ATP (1 mM) and Npl3 (47 μM). As shown in Table 1, the K_I values obtained for the various nucleotides correspond closely to the K_d values obtained via equilibrium fluorescence. These studies demonstrate that the displacement assay can be used to measure the real binding affinities of natural nucleotides in the absence of substrate turnover.

Table 1: Dissociation and Inhibition Constants for Sky1pΔNS and Various Nucleotides[a]

	Sky1pΔNS	
nucleotide	K_d (μM)	K_I (μM)
ADP	43 ± 6	45 ± 5
ATP	2000 ± 300	
MANT-ATP	12 ± 1.5	
MANT-ADP	13 ± 3	
adenosine	1000 ± 100	1000 ± 90
AMP	730 ± 65	650 ± 75
AMPPNP	650 ± 50	700 ± 85

[a] The dissociation and inhibition constants were measured in 50 mM Mops buffer (pH 7) using 4 mM free Mg^{2+} at 23 °C. Dissociation constants were derived using eqs 1 and 2, and inhibition constants were derived using eq 3.

Table 2: Dissociation constants for ADP and ATP in the Absence and Presence of Mg^{2+} for Sky1pΔNS and PKA[a]

	Sky1pΔNS		PKA	
nucleotide	(+) Mg^{2+}	(−) Mg^{2+}	(+) Mg^{2+}	(−) Mg^{2+}
ADP	43 ± 6[b]	47 ± 7	50 ± 7	350 ± 50
ATP	2000 ± 300[b]	2500 ± 350	43 ± 6	420 ± 55
MANT-ADP	12 ± 1.5[b]	15 ± 2	18 ± 2	190 ± 18

[a] Dissociation constants were measured in 50 mM Mops buffer (pH 7) using either no Mg^{2+} (−) or 4 mM free Mg^{2+} for Sky1p and 10 mM free Mg^{2+} for PKA (+) at 23 °C. Dissociation constants were derived using eqs 1 and 2. [b] Data taken from Table 1.

Domain Insert in Sky1p Does Not Alter Nucleotide Binding. All SRPKs possess domain inserts (approximately 250 residues) in the kinase domain (*26*). Binding studies were performed to determine whether this insert in full-length Sky1p changes the properties of the nucleotide binding pocket relative to the core kinase domain. Unlike Sky1pΔNS, we could not obtain pure fractions of the full-length enzyme at high concentrations to perform detailed fluorescence studies. Instead, several important steady-state kinetic parameters were measured for comparison with the truncated enzyme. Using saturating amounts of Npl3 (47 μM), the K_m for ATP and the K_I for ADP were measured and found to be 235 ± 40 and 70 ± 10 μM, respectively. These values are similar to previously published K_I and K_m values for Sky1pΔNS (K_m = 200 μM and K_I = 45 μM) (*24*). Given these similarities, it is unlikely that the domain insert influences nucleotide binding in Sky1p.

*Magnesium Does Not Enhance Nucleotide Affinity in Sky1p*ΔNS. To assess the role of Mg^{2+} in modulating the affinity of the natural nucleotides, displacement assays were performed in the absence and presence of the metal activator. In these experiments, Sky1pΔNS (1 μM) is preequilibrated with either ADP (100 μM) or ATP (1 mM) in the absence of Mg^{2+} prior to the addition of increasing concentrations of MANT-ADP (Figure 5A). As a control for these assays, we measured the $K_d^{MANT-ADP}$ values in the presence and absence of Mg^{2+} and found them to be very similar (Table 2). Using eq 2, K_d values for ADP and ATP of 47 ± 7 and 2500 ± 350 μM, respectively, were then calculated in the absence of Mg^{2+} (Table 2) using the changes in apparent affinity of MANT-ADP at fixed concentrations of the natural nucleotides. The $^{app}K_d$ values for MANT-ADP in the presence of ADP and ATP (Figure 5A) are 47 ± 9 and 21 ± 3 μM, respectively. As explained previously, the K_d^{ATP} is known with less accuracy than the other nucleotides owing to the high concentration of ATP needed to displace the MANT nucleotide. Overall, the presence of Mg^{2+} does not enhance the binding affinities of MANT-ADP, ATP, or ADP (Table 2).

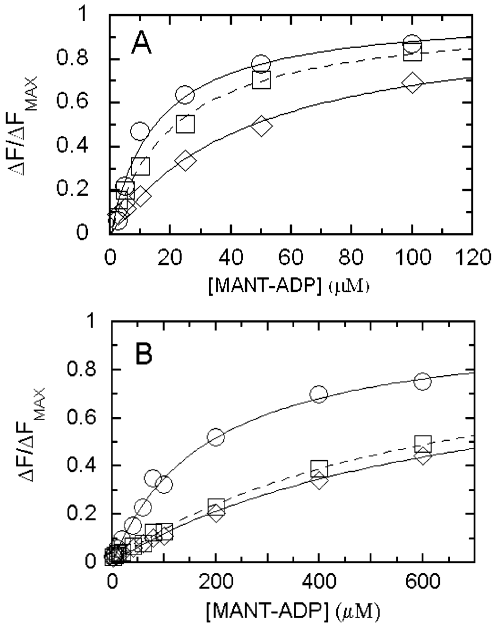

FIGURE 5: Effects of Mg^{2+} on nucleotide binding for Sky1p and PKA. (A) Sky1pΔNS. Relative changes in MANT-ADP fluorescence at 440 nm upon the association with Sky1pΔNS in the absence of Mg^{2+} is monitored in the absence (○) and presence of 100 M ADP (◇) and 1 mM ATP (□). (B) PKA. Relative changes in MANT-ADP fluorescence at 440 nm upon association with PKA in the absence of Mg^{2+} is monitored in the absence (○) and presence of 1 mM ADP (◇) and 1 mM ATP (□). The data were fit to eq 1, and natural nucleotide K_d vlaues were determined using eq 2 and are listed in Table 2.

Nucleotide Binding to PKA Is Metal Dependent. To determine whether the ability of Sky1pΔNS to bind to natural nucleotides in the absence of Mg^{2+} is specific to SRPKs, or is a general phenomenon of other protein kinases, we measured the affinities of nucleotides to PKA in the presence and absence of Mg^{2+}. By preequilibrating PKA (1 μM) with either ADP (200 μM) or ATP (200 μM) in the presence of 10 mM free Mg^{2+} prior to the addition of increasing concentrations of MANT-ADP, K_d values for ADP and ATP of 50 ± 7 and 43 ± 6 μM, respectively, were obtained using eq 2 (Table 2). The $^{app}K_d$ values for MANT-ADP in the presence of Mg^{2+} and ADP and ATP are 90 ± 10 and 100 ± 15 μM, respectively. A determination of the nucleotide K_d values in the absence of Mg^{2+} was then carried out in a similar fashion in which PKA (1 μM) is preequilibrated with either ADP (1 mM) or ATP (1 mM) in the absence of Mg^{2+} prior to the addition of increasing concentrations of MANT-ADP. The observed competition curves, shown in Figure 5B, were then used to obtain K_d values for ADP and ATP of 350 ± 50 and 420 ± 55 μM, respectively (Table 2). K_d values for MANT-ADP in the presence of 10 mM free Mg^{2+} and in the absence of Mg^{2+} for PKA are 18 ± 2 and 190 ± 18 μM, respectively (Table 2). In the absence of Mg^{2+}, the $^{app}K_d$ values for MANT-ADP in the presence of ADP and ATP are 730 ± 100 and 640 ± 85 μM, respectively. Thus, the presence of Mg^{2+} enhances the affinity of nucleotides by approximately 10-fold in PKA, whereas this physiological

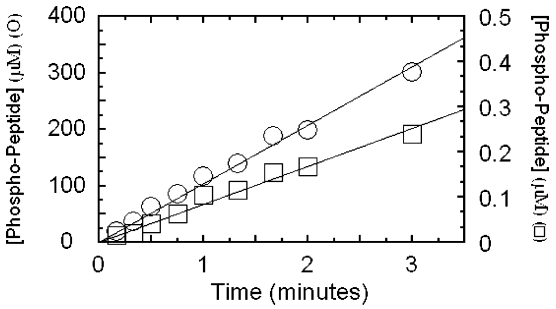

FIGURE 6: Time-dependent incorporation of phosphate into the peptide YRTRDAPRERSPTR (2 mM) in the presence and absence of Mg^{2+}. Assays were performed using 1 μM Sky1pΔNS and either 2 mM ATP in the absence (□) and presence (○) of 4 mM free Mg^{2+}.

metal has no impact on nucleotide binding in Sky1pΔNS (Table 2).

Magnesium Facilitates the Rate of Phosphoryl Transfer in Sky1pΔNS. Since Mg^{2+} does not influence the binding properties of nucleotides to Sky1p (Table 2), we determined the extent to which the metal influences catalysis. The effects of Mg^{2+} on the phosphorylation of the synthetic peptide substrate YTRDAPRERSPTR were measured using activity assays. These experiments were carried out by monitoring the time-dependent incorporation of ^{32}P from [γ-^{32}P] ATP (2 mM) into a fixed amount of substrate peptide (2 mM) by Sky1pΔNS (1 μM) in the absence and presence of 4 mM free Mg^{2+} (Figure 6). In the absence and presence of Mg^{2+}, the observed rate constants were 0.08 ± 0.008 and 100 ± 6 min^{-1}, respectively. These data show that the presence of Mg^{2+} leads to a 1300-fold increase in the turnover rate. Thus, while Mg^{2+} has no effect on ATP or ADP binding, it plays a significant role in positioning/stabilizing the phosphate for efficient phosphoryl group transfer in Sky1pΔNS.

DISCUSSION

In the past decade, it has become apparent that the nucleotide pocket is a key region in the active site for regulating function in protein kinases. Fast mixing techniques reveal that ADP release is rate limiting in PKA (*31*, *37*, *38*) and other protein kinases (*39*, *40*). Thus, activity control through regulatory proteins or posttranslational modifications is likely to involve changes in nucleotide and kinase dissociation, the rate-limiting event in protein phosphorylation (*41*). Current anti-kinase drug strategies are now directed at the nucleotide pocket. Selectivity among these small inhibitors is achieved through the careful exploitation of subtle differences between the nucleotide pockets within the enzyme family (*7*). The phosphorylation of several protein kinases appears to regulate catalysis by remodeling parts of the nucleotide pocket, particularly residues near the triphosphoryl region of ATP. In one example, phosphorylation of the insulin receptor kinase leads to movements in helix C, a translation that indirectly strengthens electrostatic interactions with ATP and positions the γ phosphate for productive phosphoryl group transfer (*42*).

Given the significance of nucleotide binding for catalytic regulation in protein kinases, it is surprising that there are few structure−function studies on nucleotide selectivity. Such studies could offer useful insights into how nucleotide stabilization facilitates the rate of substrate phosphorylation in the active site. In general, there are many steady-state kinetic analyses of protein kinases, but these studies typically do not provide any direct information on the real binding affinity of ATP or substrate (*41*). In one example, we showed that the K_d for a substrate peptide to PKA is about 2 orders of magnitude larger than the corresponding K_m (*31*), underscoring the need for techniques that directly measure ligand binding affinities in the absence of substrate turnover. Although fluorescent MANT analogues have been used previously to measure binding affinities (*43*, *44*), derivatization leads to a modified nucleotide that binds unproductively to Sky1p (Figure 3). Furthermore, the addition of MANT to ATP increases the affinity of the derivative by approximately 2 orders of magnitude as compared to ATP (Table 1). These findings make it difficult to use the MANT compounds as mimics of the natural nucleotides. In this report, we have circumvented this limitation of fluorescent derivatives by using the good affinities of the MANT compounds in displacement assays to measure the dissociation constants of natural nucleotides that differ by substitution at the ribose ring.

Sky1p Sensitively Discriminates between ATP and ADP. By monitoring the degree to which various nucleotides displace MANT derivatives from the active site of Sky1p, dissociation constants were calculated from perturbations in the apparent affinity of the derivative (Table 1). In these experiments, we showed that Sky1p binds the product, ADP, preferentially over ATP by a factor of approximately 50, whereas PKA binds both nucleotides with similar affinities (Table 1). Thus, the phosphate of ATP strongly destabilizes nucleotide binding in Sky1p by 2.3 kcal/mol. The molecular basis of this selectivity can be explained by the recent X-ray structures of Sky1p with ATP and ADP bound (*33*). As shown in Figure 7, the binding of ADP appears to cause greater closure of the pocket relative to ATP, allowing ADP to make three hydrogen bonds at the bottom of the pocket between the 2′- and the 3′-hydroxyl oxygens and the side chain of Asn252 and between the 3′-OH and the backbone carbonyl oxygen of Glu298. ATP forms only one hydrogen bond between 3′-OH and Asn252. Moreover, the ADP-containing structure exhibits greater lobe rotation and a downward movement of the entire glycine-rich loop, creating a tighter fit for the product nucleotide as well as more hydrogen bonding between the phosphates and the kinase. In contrast, the ATP-containing structure shows that the phosphate oxygens of ATP are positioned too high in the active-site cleft to accept a hydrogen bond from the conserved lysine in strand 3. By comparison, crystallographic structures of PKA with ATP or ADP bound show no significant changes in hydrogen bonding or lobe movements (*45*). Accordingly, PKA does not discriminate between ATP and ADP in our displacement assay (Table 2).

Unique Topology of the Triphosphoryl Region of Sky1p. Unlike PKA, Sky1p displays exquisite selectivity for ATP and ADP. To better understand the origins of this selectivity, we determined the dissociation constants for several nucleotides that differ by the number of phosphates attached to the ribose ring (adenosine (Ad), AMP, and the ATP analogue AMPPNP). As shown in Table 1, the dissociation constants for these nucleotides indicate that the β-phosphate of ADP is important for high affinity binding in Sky1p, whereas the α- and γ-phosphates are not. This finding is displayed

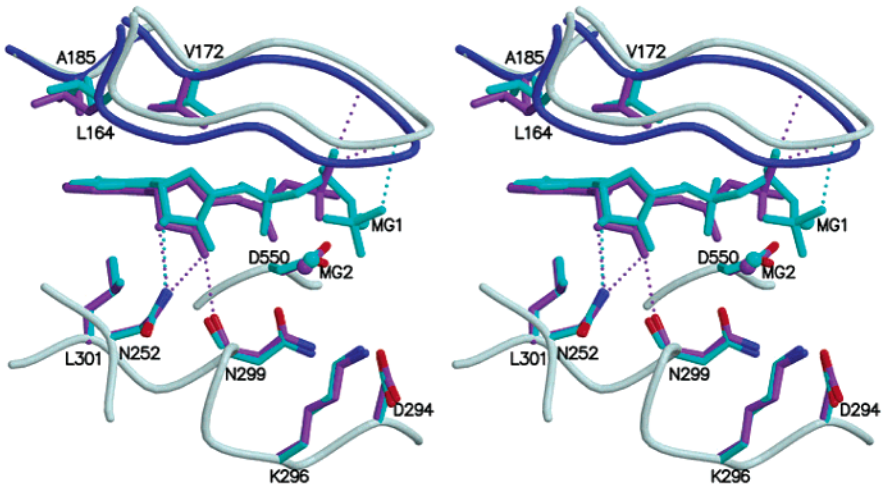

FIGURE 7: Stereodiagram showing ADP and ATP binding pocket of Sky1ΔNS. Cα tube representations for the nucleotide binding pockets of the ADP bound structure (blue Cα tube and purple residues) and the ATP bound structure (gray Cα tube and cyan residues) are overlaid. Hydrogen bonds are shown as dotted lines. The structural data are taken from ref *33*.

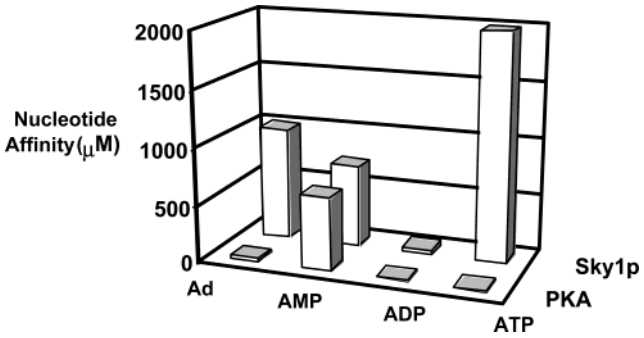

FIGURE 8: Binding affinities of Ad, AMP, ADP, and ATP for Sky1p and PKA. The binding affinities are expressed in terms of K_d. The data for Sky1pΔNS were taken from Table 1 whereas the data for PKA were taken from ref *47*.

graphically in Figure 8, where the nucleotide binding affinities are compared for Sky1p and PKA. For PKA, the addition of the α-phosphate to the ribose destabilizes the enzyme−nucleotide interaction by 20-fold. In this kinase, the subsequent addition of the β- and γ-phosphates has no effect on nucleotide binding relative to adenosine, suggesting that the repulsive interaction at the α-phosphate subsite is compensated by additional phosphates. In blunt contrast, the addition of the α-phosphate does not significantly impair the nucleotide binding affinity in Sky1p relative to adenosine. The differences in affinity of adenosine for the two kinases (>10-fold) suggest that they stabilize the nucleotide in different manners. In PKA, high affinity nucleotide binding appears encoded in the contacts made with the adenosine region, whereas Sky1p relies on the β-phosphate for the high affinity binding of ADP. Curiously, while Sky1p and PKA provide substantially different environments for the phosphate, the rates of phosphoryl transfer in the active sites of both enzymes are fast and do not limit substrate turnover (*24*, *31*).

Dual versus Single Function Metals. Protein kinases typically bind two magnesium ions in the active site to support substrate phosphorylation (*41*). It has been traditionally held that these metals provide two essential functions. Chelation of the triphosphoryl region is thought to improve ATP binding affinity and stabilize the charge in the reaction transition state, thereby facilitating rapid substrate phosphorylation (*46*). PKA adequately fits this dual function model since no appreciable substrate phosphorylation is observed in the absence of Mg^{2+} (*47*), and the K_d values for ATP and ADP are substantially lower in the presence of metal (Table 2). X-ray diffraction studies reveal that both metals make important contacts with the nonbridging oxygen of the ATP phosphate and residues in the active site of PKA, supporting the more efficient binding of nucleotide in the presence of activator (*48*). While Mg^{2+} is certainly important for enhancing the rate of substrate phosphorylation in Sky1p (Figure 6), it has no real effect on the affinity of ATP or ADP. These findings not only further emphasize key differences in the nucleotide binding pocket between Sky1p and PKA but also indicate that the role of the metals may vary within the kinase family. While PKA favors a dual function mechanism for Mg^{2+}, Sky1p appears to employ a single function for this activator.

Nucleotide Binding and Catalysis. Prior steady-state kinetic analyses demonstrated that Sky1p binds to ATP with low apparent affinity (high K_m values) as compared to the prototype serine/threonine kinase, PKA [K_m = 200 μM for Sky1p vs 10 μM for PKA (*24*, *49*)]. The fluorescence displacement assays now show that this high K_m is due to the poor binding properties of ATP in the nucleotide pocket (K_d = 2000 μM). The 10-fold discrepancy between K_m and K_d may reflect the fast rate of phosphoryl transfer in the active site as compared to other kinetic steps. By analyzing the individual steps in the PKA reaction, we showed that the K_m for a peptide substrate is approximately 20-fold lower than K_d owing to a fast phosphoryl transfer rate (500 s^{-1}) as compared to slow product release (20 s^{-1}) (*31*). For Sky1p, we measured a similar relationship between the rates of phosphoryl transfer and product release (*24*). Thus, we anticipate that the difference between K_m and K_d for ATP in the steady-state kinetic and fluorescence displacements assays is not likely to be the result of positive binding synergism between nucleotide and substrate but is more likely to reflect a kinetic phenomenon resulting from the fast chemical event in the active site.

It is widely believed that protein kinases support rapid phosphoryl transfer by metal chelation of the nonbridging oxygen of the ATP γ phosphate (*46*, *48*, *50*, *51*). For PKA,

metal binding not only supports substrate phosphorylation but also assists ATP binding (Table 2). On the other hand, the results for Sky1p present an interesting dilemma for this model since fast phosphoryl transfer in this kinase is achieved through destabilization of the phosphate. While the binding and structural studies do not provide a direct solution, it is noteworthy that one of the active-site metals in Sky1p (Mg1 in Figure 7) interacts with the bridging oxygen rather than the nonbridging oxygen, as observed in other kinases. Both experimental and theoretical investigations suggest that protein kinases utilize a dissociative mechanism where bond breaking between the bridging oxygen and phosphorus precedes bond formation with the serine hydroxyl oxygen in the reaction transition state (*52*−*55*). Such a mechanism would be greatly facilitated by metal stabilization of the developing negative charge on the ADP leaving group (*41*). It is compelling to speculate that the Mg^{2+} in the active site of Sky1p with its atypical placement near the bridging oxygen may serve this unique function.

REFERENCES

1. Klein, P. S., and Melton, D. A. (1996) *Proc. Natl. Acad. Sci. U.S.A. 93*, 8455−9.
2. Burk, D. L., and Berghuis, A. M. (2002) *Pharmacol. Ther. 93*, 283−92.
3. Fabbro, D., Ruetz, S., Buchdunger, E., Cowan-Jacob, S. W., Fendrich, G., Liebetanz, J., Mestan, J., O'Reilly, T., Traxler, P., Chaudhuri, B., Fretz, H., Zimmermann, J., Meyer, T., Caravatti, G., Furet, P., and Manley, P. W. (2002) *Pharmacol. Ther. 93*, 79−98.
4. Philips, A. V., and Cooper, T. A. (2000) *Cell Mol. Life Sci. 57*, 235−49.
5. De Moliner, E., Moro, S., Sarno, S., Zagotto, G., Zanotti, G., Pinna, L. A., and Battistutta, R. (2003) *J. Biol. Chem. 278*, 1831−6.
6. Cohen, P. (1999) *Curr. Opin. Chem. Biol. 3*, 459−65.
7. Fabbro, D., and Garcia-Echeverria, C. (2002) *Curr. Opin. Drug Discovery Dev. 5*, 701−12.
8. Sawyers, C. L. (2002) *Curr. Opin. Genet. Dev. 12*, 111−5.
9. Molnar-Kimber, K. L. (1996) *Transplant Proc. 28*, 964−9.
10. Stojdl, D. F., and Bell, J. C. (1999) *Biochem. Cell Biol. 77*, 293−8.
11. Tarn, W. Y., and Steitz, J. A. (1997) *Trends Biochem. Sci. 22*, 132−7.
12. Hamm, J., and Lamond, A. I. (1998) *Curr. Biol. 8*, R532−4.
13. Staley, J. P., and Guthrie, C. (1998) *Cell 92*, 315−26.
14. Yeakley, J. M., Tronchere, H., Olesen, J., Dyck, J. A., Wang, H. Y., and Fu, X. D. (1999) *J. Cell Biol. 145*, 447−55.
15. Prasad, J., Colwill, K., Pawson, T., and Manley, J. L. (1999) *Mol. Cell Biol. 19*, 6991−7000.
16. Cao, W., Jamison, S. F., and Garcia-Blanco, M. A. (1997) *RNA 3*, 1456−67.
17. Mermoud, J. E., Cohen, P. T., and Lamond, A. I. (1994) *EMBO J. 13*, 5679−88.
18. Colwill, K., Pawson, T., Andrews, B., Prasad, J., Manley, J. L., Bell, J. C., and Duncan, P. I. (1996) *EMBO J. 15*, 265−75.
19. Duncan, P. I., Stojdl, D. F., Marius, R. M., Scheit, K. H., and Bell, J. C. (1998) *Exp. Cell Res. 241*, 300−8.
20. Gui, J. F., Tronchere, H., Chandler, S. D., and Fu, X. D. (1994) *Proc. Natl. Acad. Sci. U.S.A. 91*, 10824−8.
21. Wang, H. Y., Lin, W., Dyck, J. A., Yeakley, J. M., Songyang, Z., Cantley, L. C., and Fu, X. D. (1998) *J. Cell Biol. 140*, 737−50.
22. Yun, C. Y., and Fu, X. D. (2000) *J. Cell Biol. 150*, 707−18.
23. Gilbert, W., Siebel, C. W., and Guthrie, C. (2001) *RNA 7*, 302−13.
24. Aubol, B. E., Nolen, B., Vu, D., Ghosh, G., and Adams, J. A. (2002) *Biochemistry 41*, 10002−9.
25. Siebel, C. W., Feng, L., Guthrie, C., and Fu, X. D. (1999) *Proc. Natl. Acad. Sci. U.S.A. 96*, 5440−5.
26. Nolen, B., Yun, C. Y., Wong, C. F., McCammon, J. A., Fu, X. D., and Ghosh, G. (2001) *Nat. Struct. Biol. 8*, 176−83.
27. Andersen, M. D., Shaffer, J., Jennings, P. A., and Adams, J. A. (2001) *J. Biol. Chem. 276*, 14204−14211.
28. Hubbard, S. R. (1997) *EMBO J. 16*, 5572−81.
29. Jeffrey, P. D., Russo, A. A., Polyak, K., Gibbs, E., Hurwitz, J., Massague, J., and Pavletich, N. P. (1995) *Nature 376*, 313−20.
30. Cole, P. A., Burn, P., Takacs, B., and Walsh, C. T. (1994) *J. Biol. Chem. 269*, 30880−7.
31. Grant, B. D., and Adams, J. A. (1996) *Biochemistry 35*, 2022−9.
32. Prowse, C. N., Hagopian, J. C., Cobb, M. H., Ahn, N. G., and Lew, J. (2000) *Biochemistry 39*, 6258−66.
33. Nolen, B., Ngo, J., Chakrabarti, S., Vu, D., Adams, J. A., and Ghosh, G. (2003) *Biochemistry 42*, 9575−85.
34. Adams, J. A., and Taylor, S. S. (1992) *Biochemistry 31*, 8516−22.
35. Gill, S. C., and von Hippel, P. H. (1989) *Anal. Biochem 182*, 319−26.
36. Remmers, A. E., Posner, R., and Neubig, R. R. (1994) *J. Biol. Chem. 269*, 13771−8.
37. Lew, J., Taylor, S. S., and Adams, J. A. (1997) *Biochemistry 36*, 6717−24.
38. Zhou, J., and Adams, J. A. (1997) *Biochemistry 36*, 15733−8.
39. Shaffer, J., Sun, G., and Adams, J. A. (2001) *Biochemistry 40*, 11149−55.
40. Jan, A. Y., Johnson, E. F., Diamonti, A. J., Carraway, I. K., and Anderson, K. S. (2000) *Biochemistry 39*, 9786−803.
41. Adams, J. A. (2001) *Chem. Rev. 101*, 2271−2290.
42. Hubbard, S. R., Wei, L., Ellis, L., and Hendrickson, W. A. (1994) *Nature 372*, 746−54.
43. Ni, Q., Shaffer, J., and Adams, J. A. (2000) *Protein Sci. 9*, 1818−27.
44. Plesniak, L., Horiuchi, Y., Sem, D., Meinenger, D., Stiles, L., Shaffer, J., Jennings, P. A., and Adams, J. A. (2002) *Biochemistry 41*, 13876−82.
45. Madhusudan, Trafny, E. A., Xuong, N. H., Adams, J. A., Ten Eyck, L. F., Taylor, S. S., and Sowadski, J. M. (1994) *Protein Sci. 3*, 176−87.
46. Adams, J. A., and Taylor, S. S. (1993) *Protein Sci. 2*, 2177−86.
47. Bhatnagar, D., Roskoski, R., Rosendahl, M. S., and Leonard, N. J. (1983) *Biochemistry 22*, 6310−7.
48. Zheng, J., Knighton, D. R., Ten Eyck, L. F., Karlsson, R., Xuong, N., Taylor, S. S., and Sowadski, J. M. (1993) *Biochemistry 32*, 2154−61.
49. Cook, P. F., Neville, M. E., Jr., Vrana, K. E., Hartl, F. T., and Roskoski, R., Jr. (1982) *Biochemistry 21*, 5794−9.
50. Huang, C. Y., Yuan, C. J., Luo, S., and Graves, D. J. (1994) *Biochemistry 33*, 5877−83.
51. Mildvan, A. S. (1997) *Proteins 29*, 401−16.
52. Valiev, M., Kawai, R., Adams, J. A., and Weare, J. H. (2003) *J. Am. Chem. Soc. 125*, 9926−7.
53. Zhou, J., and Adams, J. A. (1997) *Biochemistry 36*, 2977−84.
54. Kim, K., and Cole, P. A. (1998) *J. Am. Chem. Soc. 119*, 11096−7.
55. Ablooglu, A. J., Till, J. H., Kim, K., Parang, K., Cole, P. A., Hubbard, S. R., and Kohanski, R. A. (2000) *J. Biol. Chem. 275*, 30394−8.

BI035200C